Contents lists available at ScienceDirect

Toxicon

MicroRNA-mRNA expression profiles and functional network after injection of botulinum toxin type A into submandibular glands

Qian-Ying Mao [a], Shang Xie [a], Li-Ling Wu [b], Ruo-Lan Xiang [b,*], Zhi-Gang Cai [a,**]

[a] Department of Oral and Maxillofacial Surgery, Peking University School and Hospital of Stomatology, Beijing, 100081, China
[b] Department of Physiology and Pathophysiology, Peking University School of Basic Medical Sciences, Key Laboratory of Molecular Cardiovascular Sciences, Ministry of Education, Beijing, 100191, China

ARTICLE INFO

ABSTRACT

Botulinum toxin type A (BTXA) is effective for the treatment of sialorrhea. MicroRNAs (miRNAs) have significant functions in salivary diseases, but the role of miRNAs during BTXA-inhibited salivary secretion is not yet clear. A total of 19 differentially expressed (DE) miRNAs and 1072 DE mRNAs were identified following BTXA injected into submandibular glands of rats (n = 4) through miRNA sequencing and microarray analysis. Bioinformatic analysis identified that several pathways may be associated with the inhibition of salivary secretion, such as the MAPK signalling pathway, tight junctions, and cytokine-cytokine receptor interaction. We predicted the target genes of DE miRNAs and established the miRNA-mRNA interaction network. The intersection of DE mRNAs and target genes of DE miRNAs was performed and seven mRNAs were obtained: Egr2, Paqr9, Zkscan1, Usp6n, Cyb561a3, Zfhx4, and Clic5. These findings explore the mechanism of BTXA in inhibiting salivary secretion and probably will provide new ideas for clinical application.

1. Introduction

Sialorrhea is a syndrome of excessive salivary gland secretion or dysphagia resulting in excessive salivation or frequent discomfort with swallowing. This condition is one of the common complications of several neurological disorders, such as cerebral palsy, Parkinson's disease, and amyotrophic lateral sclerosis (Barbero et al., 2016). Although sialorrhea is not a life-threatening disease, the resulting physiological and psychosocial sequelae can have a significant negative impact on the quality of life of patients and caregivers. Too much saliva can lead to social awkwardness and may worsen depressive symptoms. Saliva that remains in the mouth can become inhaled, leading to suffocation and pneumonia (Srivanitchapoom et al., 2014). Clinically, sialorrhea can be treated in several ways, such as surgery, behaviour therapy, and drugs. However, surgery and radiation therapy can cause serious complications, and the use of anticholinergic drugs will cause systemic side effects. Therefore, it is necessary to look for a safe and effective treatment with fewer side effects (Banfi et al., 2015; Walshe et al., 2012).

Botulinum toxin type A (BTXA) is a neurotoxin produced by Clostridium botulinum during growth and reproduction. Based on a number of clinical studies, it has been reported that intraglandular injection of BTXA is safe and effective for treating sialorrhea (Restivo et al., 2018), but this treatment also causes some side effects such as dry mouth and difficulty swallowing. However, the reasons for these side effects are still unclear which limits the clinical use of BTXA. BTXA is generally considered to inhibit salivary secretion by suppressing the parasympathetic nervous system through inhibiting the release of acetylcholine (Slawek and Madalinski, 2017). However, our previous studies showed that BTXA has direct functions in acinar cells, redistribution of aquaporin 5 (Xu et al., 2015), and inhibition of autophagic flux (Xie et al., 2019). A deeper understanding of these phenomena could improve the mechanism of BTXA inhibition of salivary secretion, thereby making it more effective to treat diseases such as sialorrhea and other glandular hypersecretory diseases.

MicroRNAs (miRNAs) are noncoding RNAs with a size of approximately 21–23 nucleotides that are usually embedded into the 3′- untranslated region of target genes, negatively regulating the expression of target genes at the transcriptional or posttranscriptional level (Mohr and Mott, 2015). In addition, miRNAs have been reported to be extensively

* Corresponding author. Department of Physiology and Pathophysiology, Peking University School of Basic Medical Sciences, Key Laboratory of Molecular Cardiovascular Sciences, Ministry of Education, No. 38 Xueyuan Road, Haidian District, Beijing, 100191, China.
** Corresponding author. Department of Oral and Maxillofacial Surgery, Peking University School and Hospital of Stomatology, No. 22 Zhong Guan Cun South Street, Haidian District, Beijing, 100081, China.
E-mail addresses: xiangrl@bjmu.edu.cn (R.-L. Xiang), c2013xs@163.com (Z.-G. Cai).

involved in the development of salivary gland disease. MiR-200b-5p detected in the small salivary glands of patients with Sjögren's syndrome can be used as a novel strong molecular biomarker for the development of non-Hodgkin's lymphoma (Kapsogeorgou et al., 2018). Salivary cystatin S may be a marker of primary Sjögren's syndrome, and an upregulation of miR-126 and miR-335-5p might be implicated in salivary cystatin S expression (Martini et al., 2017). MiR-181a plays an important role in the metastasis of salivary adenoid cystic carcinoma by regulating the MAPK-Snai2 pathway (He et al., 2013). The down-regulation of miR-1207-5p and miR-4695-3p results in elevated tripartite motif protein 21 levels in the small salivary gland, leading to the occurrence of Sjogren's syndrome (Yang et al., 2016). Therefore, miRNAs play an important role in the occurrence and development of salivary diseases, as well as in regulating the functions of salivary glands.

In current studies, it has been found that BTXA can affect the expression of miRNAs and thereby affect their function. For example, miR-133a/b and miR-1/206 play a role in BTXA -induced muscle paralysis (Worton et al., 2018). BTXA could inhibit human skin keloid fibroblast proliferation and migration and promote apoptosis and autophagy by regulating miR-1587/miR-2392 targeted ZEB2 (Hou et al., 2019). Patients with overactive bladder injected with BTXA are found to have a low risk of urinary retention with high expression of miR-221 and miR-125b (Chermansky et al., 2018). However, to date, whether miRNA expression changes in the process of inhibiting salivary secretion triggered by BTXA has not been reported. Therefore, we investigated the miRNA and mRNA expression profiles after injection of BTXA into the submandibular glands of rats using RNA-seq and microarray analysis. We also constructed a miRNA-mRNA interaction network to identify the possible mechanisms. The aim of this study is to further explore the mechanism of BTXA's role in inhibiting salivary secretion, and provide new ideas for clinical application.

2. Materials and methods

2.1. Experimental animals

The SD rats were anesthetized, and the left submandibular gland was exposed by a median cervical incision. The control group was injected with 0.1 ml normal saline. The BTXA group was injected with 6 U BTXA (Lanzhou Biological Co, China) dissolved in 0.1 ml normal saline. The wound was sutured postoperatively. Two weeks later, a midline incision of the neck was made with a scalpel and the submandibular gland was dissected free from the fat and connective tissue. Then, we separated the sublingual gland and cut off the duct and the running paralleled artery. Finally, the submandibular gland was removed in liquid nitrogen and then transferred to −80 °C.

We used four rats in each group for preparing the sample of RNA-seq and microarray analysis. As for the validation experiment, we used five to seven rats in each group. All procedures were approved by the Ethics Committee for Animal Research, Peking University Health Science Centre (LA2020067), and complied with the Guide for the Care and Use of Laboratory Animals (NIH Publication No. 85-23, revised 1996).

2.2. RNA-seq and microarray analysis

The miRNA sequencing libraries were prepared and the library quality was determined using the Agilent 2100 Bioanalyzer. The libraries were denatured as single-stranded DNA and sequenced for 51 cycles on an Illumina NextSeq500 according to the manufacturer's instructions. The purified libraries were quantified using the Agilent High Sensitivity DNA Kit (Agilent Technology, USA) and their size distribution was also confirmed. Known miRNA quantification and novel miRNA prediction were performed using miRDeep2 software.

The Rat 4 × 44K Gene Expression Array was used to detect the full coverage of rat genes and transcripts. Sample labelling and array hybridization were carried out according to the Agilent One-Colour Microarray-Based Gene Expression Analysis protocol (Agilent Technology, USA). We used Agilent Feature Extraction software (version 11.0.1.1) to obtain the array images. Gene Spring GX v12.1 software (Agilent Technology, USA) was used to process the subsequent data to acquire differentially expressed (DE) mRNAs.

The RNA-Seq data have been deposited in the NCBI (National Center for Biotechnology Information) Gene Expression Omnibus (GEO) and the accession number is GSE141815. The microarray data have also been deposited in NCBI GEO and the accession number is GSE141819.

2.3. Gene Ontology and Kyoto Encyclopedia of Genes and Genomes pathway analysis

Gene Ontology (GO) analysis included 3 categories: molecular function, cell composition and biological process. Fisher's exact test was used to calculate the correlation between DE genes and functional items, which was reflected by the *p*-value. In addition, Kyoto Encyclopedia of Genes and Genomes (KEGG) database was used to analyse the possible biological pathways in which DE genes might be involved, and *p*-value ≤ 0.05 was used as the significance threshold.

2.4. Establishment of miRNA-mRNA network

The two databases mirdbV6 (http://mirdb.org/mirdb/) and Taregetscan 7.1 (http://www.targetscan.org/mmu_71/) were used to predict the target genes of DE miRNAs, and Cytoscape (v2.8.3) was used to

depict the network. In the miRNA-mRNA network, a circular node represents mRNA, a rectangular node represents miRNA, and the association between them is plotted in solid lines.

2.5. Quantitative real-time reverse transcription-polymerase chain reaction (qRT-PCR)

TRIzol RNA Reagent (Invitrogen, USA) was used to extract the total RNA according to the manufacturer's instructions. Then cDNA was synthesized from 2 μg RNA using a RevertAid First Strand cDNA Synthesis Kit (Promega, USA). The qRT-PCR experiments were performed using a DyNAmo Color Flash SYBR Green qPCR Kit on Thermo PikoReal PCR Systems (Thermo Fisher Scientific, USA). To detect miRNA

expression levels, we used the miDETECT A Track miRNA qRT-PCR Starter Kit (RiboBio Co, China) for reverse transcription and qRT-PCR experiments. U6 and β - actin were used as the internal controls to detect miRNA and mRNA, respectively. The relative gene expression was analyzed by the $2^{-\Delta\Delta Ct}$ method. The primer sequences are listed in Supplementary Table S1.

2.6. Statistical analysis

Data are described as mean ± standard error of the mean. Statistical significance of the difference between control and BTXA group was evaluated using unpaired Student's t-test with GraphPad software (GraphPad Prism 7.0, USA). All p-value ≤ 0.05 were considered
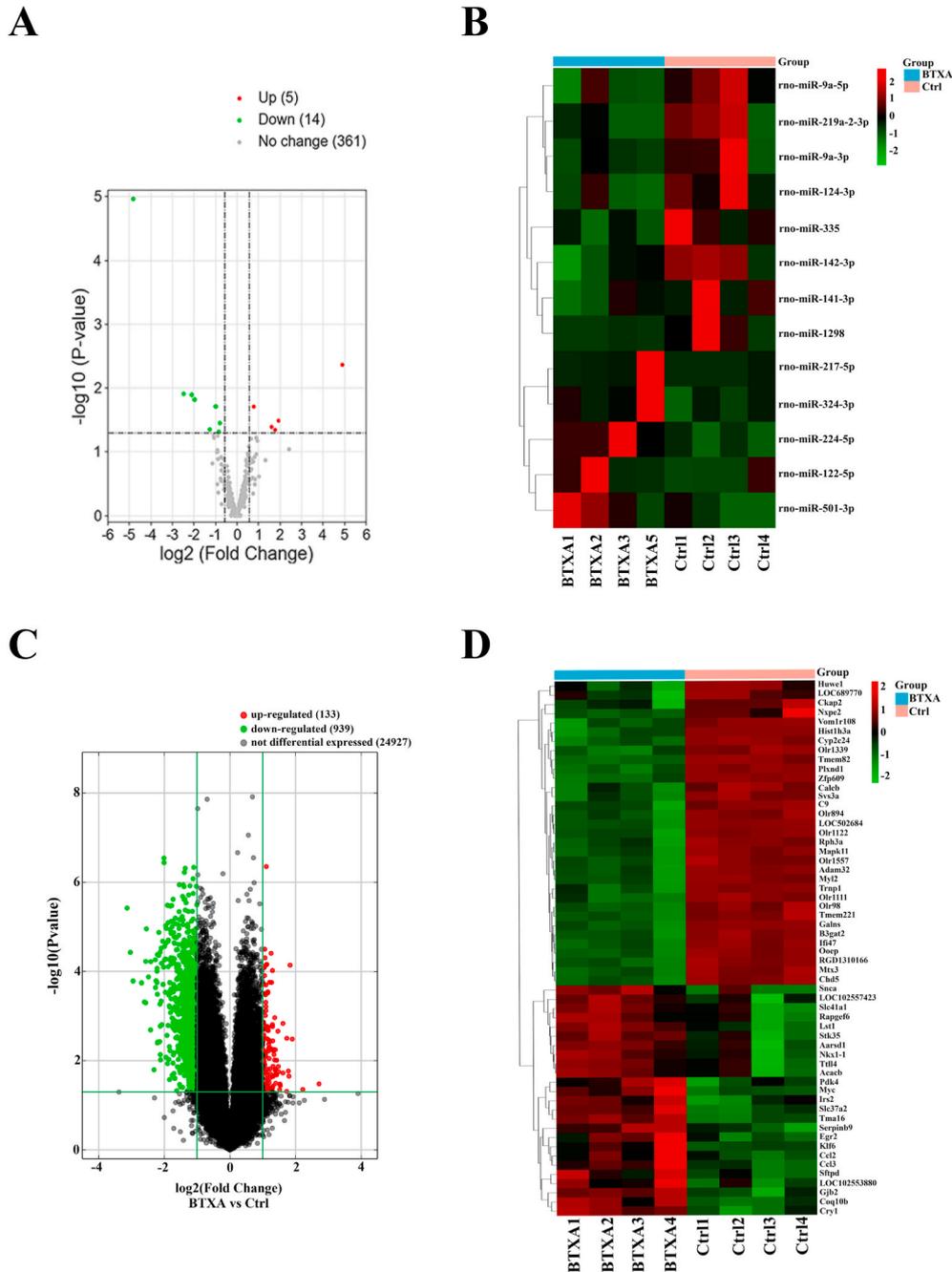
Fig. 1. Identification of DE miRNAs and mRNAs between the control group and BTXA group. (A) Volcano pots were used for identifying the DE miRNAs. (B) The heat map showed the DE miRNAs (C) Volcano pots were used for identifying the DE mRNAs. (D) The heat map showed the top 50 DE mRNAs. N = 4/group, DE, differentially expressed.

statistically significant.

3. Results

3.1. Identification of DE miRNAs and mRNAs

RNA-seq results suggested that there were only 19 DE miRNAs in the BTXA group, among which 5 were upregulated and 14 were down-regulated, as shown in the volcano plot (Fig. 1A) and the cluster diagram (Fig. 1B). The details of the 19 DE miRNAs are shown in Supplementary Table S2. The microarray results suggested that there were 1072 DE mRNAs in total, among which 133 were upregulated and 939 were downregulated, as described in the volcano plot (Fig. 1C). The cluster diagram showed the top 25 DE mRNAs that were significantly upregulated or downregulated in the BTXA group (Fig. 1D). The characteristics of the top 10 upregulated and downregulated mRNAs are shown in Supplementary Table S3.

3.2. Validation of qRT-PCR for DE miRNAs and DE mRNAs

To verify the results of high-throughput sequencing, we validated DE miRNAs and DE mRNAs (4 upregulated and 4 downregulated) with higher fold changes using qRT-PCR. As shown in Fig. 2A, rno-miR-122-5p, rno-miR-217-5p and rno-miR-224-5p were significantly upregulated; rno-miR-124-3p, rno-miR-9a-5p and rno-miR-141-3p were significantly downregulated. The mRNA expression detected by qRT-PCR showed upregulation of Ccl2, Gjb2, Ttll4 and Snca molecules and downregulation of Rph3a, Adam32, B3gat2 and Olr894 (Fig. 2B). The results from qRT-PCR validation were most consistent with the high-throughput sequencing results.

3.3. GO and KEGG analysis of DE miRNAs target genes

The target genes predicted by DE miRNAs were used for GO analysis. GO analysis of upregulated miRNA target genes showed that positive regulation of cellular metabolic process, membrane bounded organelle and identical protein binding had the highest enrichment score in the biological process, cellular component and molecular function domains, respectively (Fig. 3A). GO analysis of downregulated miRNA target genes showed that anatomical structure morphogenesis, intracellular and amide binding had the highest enrichment scores in the biological process, cellular component and molecular function domains, respectively (Fig. 3B). KEGG analysis of upregulated miRNAs target genes revealed that the main changed pathways after BTXA treatment were the Wnt signalling pathway, endocrine and other factor-regulated calcium

reabsorption, the PI3K-AKT signalling pathway, aldosterone synthesis and secretion and insulin secretion (Fig. 3C). Similarly, KEGG analysis of downregulated miRNA target genes revealed that the main enrichment pathways were focal adhesion, the MAPK signalling pathway, the PI3K-Akt signalling pathway, tight junction and the Ras signalling pathway (Fig. 3D). The characteristics of the KEGG analysis are shown in Table 1.

3.4. GO and KEGG analysis of DE mRNAs

Similarly, we also performed a GO analysis on 1072 DE mRNAs. The GO analysis of the upregulated mRNAs revealed that response to organic cyclic compound, nucleolus and cysteine-type endopeptidase inhibitor activity involved in the apoptotic process were mostly enriched in the biological process, cellular component and molecular function domains, respectively (Fig. 4A). The GO analysis of downregulated mRNAs revealed that the sensory perception, integral component of membrane and transmembrane signalling receptor activity was mostly enriched in the biological process, cellular component and molecular function domains, respectively (Fig. 4B). The KEGG analysis showed that upregulated mRNAs were involved in cytokine-cytokine receptor interaction, hepatitis B and platinum drug resistance (Fig. 4C). However, olfactory transduction, cytokine-cytokine receptor interaction and linoleic acid metabolism were obtained from the KEGG analysis of downregulated mRNAs (Fig. 4D).

3.5. Analysis of miRNA-mRNA network

Six DE miRNAs (rno-miR-9a-5p, rno-miR-124-3p, rno-miR-141-3p, rno-miR-122-5p, rno-miR-217-5p, and rno-miR-224-5p) verified by qRT-PCR were used to predict the target genes through the databases of mirdV6 and target scan7.1, and the miRNA-mRNA network was established (Fig. 5). Among them, a total of 573 target genes were predicted and the number of target genes of upregulated miRNAs was 168, and the number of downregulated miRNAs was 429. In addition, rno-miR-124-3p had the largest number of target genes, a total of 276. The details of DE miRNA target gene prediction are shown in Supplementary Table S4.

3.6. Analysis of DE miRNAs target mRNAs

A Venn diagram (Fig. 6A) demonstrates that the 573 target genes intersect with the 1072 DE mRNAs detected by microarray, and the overlapping portion are seven mRNAs (the general information is shown in Table 2). The qRT-PCR validation of these seven mRNAs was performed and the results were consistent with the microarray data, that is,
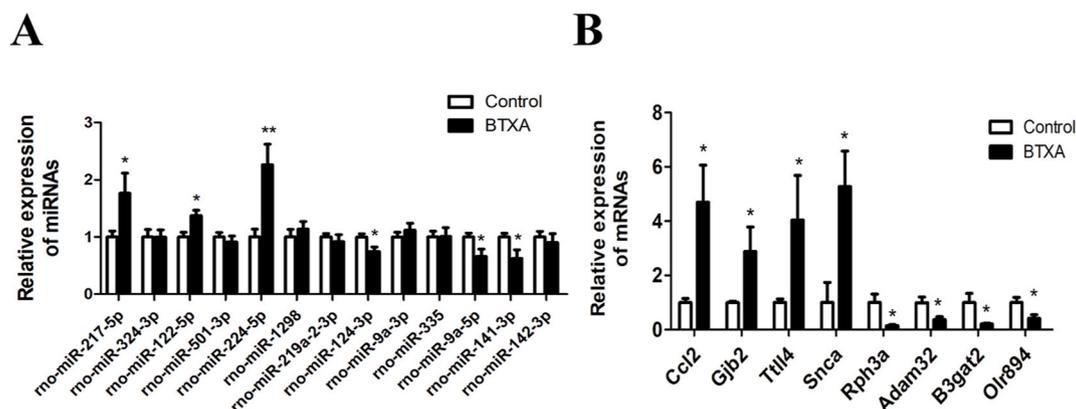
Fig. 2. Validation of DE miRNAs and mRNAs. (A) All DE miRNAs were confirmed by qRT-PCR. (B) Eight selected DE mRNAs were confirmed by qRT-PCR. U6 acted as endogenous control for miRNAs, β-actin acted as endogenous control for mRNAs. N = 5–7/group, *P < 0.05 **P < 0.01. Ccl2, C–C motif chemokine ligand 2; Gjb2, gap junction protein, beta 2; Ttll4, tubulin tyrosine ligase like 4; Snca, synuclein alpha; Rph3a, rabphilin 3A; Adam32, ADAM metallopeptidase domain 32; B3gat2, beta-1,3-glucuronyltransferase 2; Olr894, olfactory receptor 894; DE, differentially expressed.
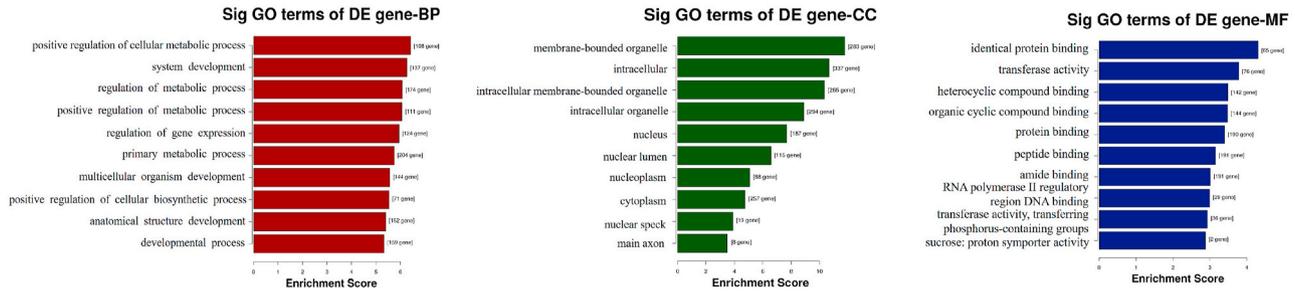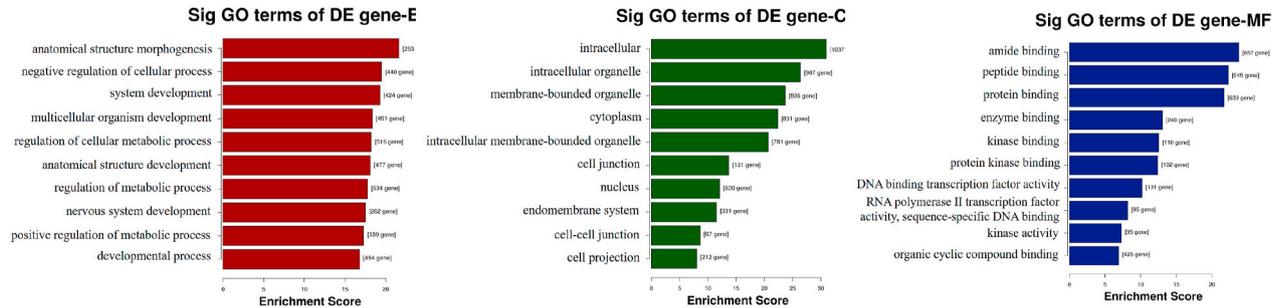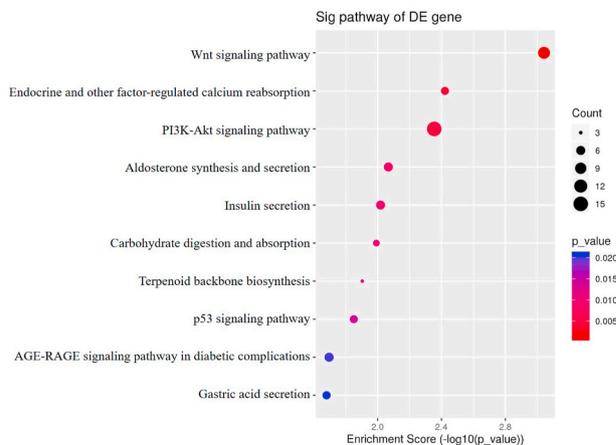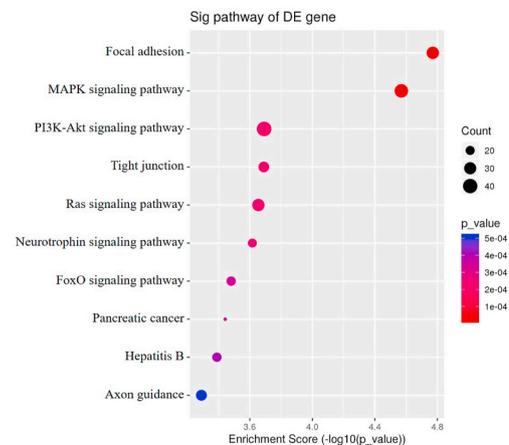
Fig. 3. GO and KEGG pathway analysis of target genes of DE miRNAs. A total of 19 DE miRNAs were chosen in GO and KEGG analysis. (A) The top 10 GOs from target genes of upregulated miRNAs. (B) The top 10 GOs from target genes of downregulated miRNAs. Top 10 pathways from a KEGG pathway analysis of target genes of upregulated miRNAs (C) and downregulated miRNAs (D). DE, differentially expressed..

Egr2, Paqr9 and Zkscan1 were upregulated, while Usp6n, Cyb561a3, Zfhx4 and Clic5 were downregulated (Fig. 6B).

4. Discussion

RNA-seq assays identified 19 DE miRNAs after the injection of BTXA into the submandibular glands, of which 5 were upregulated and 14 were downregulated. We validated rno-miR-122-5p, rno-miR-217-5p and rno-miR-224-5p as the 3 upregulated miRNAs and rno-miR-124-3p, rno-miR-9a-5p and rno-miR-141-3p as the 3 downregulated miRNAs consistent with the RNA-seq data through qRT-PCR. These six altered miRNAs are likely involved in the inhibitory effect of BTXA on salivary secretion.

We used the target genes of DE miRNAs to perform GO and KEGG analysis in order to determine the function of DE miRNAs in inhibiting salivary secretion. The KEGG analysis showed that the MAPK signalling pathway had higher enrichment (enrichment score: 4.569498466). It

has been reported that the MAPK pathway might be involved in the regulation of salivary secretion. TNF-α suppresses salivary secretion by activating the ERK1/2 pathway to reduce the expression of claudin-3 in the SMG-C6 cell line (Mei et al., 2015). Carbachol could promote salivary secretion by activating the ERK1/2 pathway to promote claudin-4 phosphorylation (Cong et al., 2015). At the same time, some research has reported that BTXA can indeed affect the MAPK pathway. BTXA can promote the production of nitric oxide, TNF-α and other proin-flammatory factors by activating the JNK, p38 and ERK1/2 pathways in macrophages (Kim et al., 2015). The botulinum toxin complex can activate the p38 pathway to increase the permeability of small intestinal epithelial cells (Miyashita et al., 2013). In combination with our high-throughput analysis, we suggested that BTXA could regulate salivary secretion by the MAPK pathway. In addition, we also found that the tight junction was highly enriched (enrichment score: 3.689473532) in our research. It has been reported that tight junctions can regulate salivary secretion by influencing paracellular pathways. For example,

Table 1
KEGG analysis of target genes predicted by DE miRNAs.

Definition	Regulation	*P*-value	Count	Enrichment score	Genes
Wnt signaling pathway	Up	<0.01	10	3.042355159	Camk2d, Cer1, Fzd4, Gpc4, Map3k7, Mapk8, Notum, Plcb1, Porcn, Smad4
Endocrine and other factor-regulated calcium reabsorption	Up	<0.01	5	2.422084847	Ap2m1, Atp1b1, Atp1b3, Dnm1, Plcb1
PI3K-Akt signaling pathway	Up	<0.01	15	2.354792076	F2r, Fgfr2, Fn1, G6pc, Ghr, Gys1, Itga6, Lamc1, Lpar1, Nr4a1, Pdgfra, Phlpp1, Pik3ca, Thbs1, Ywhaz
Aldosterone synthesis and secretion	Up	<0.01	6	2.067462179	Camk2d, Dagla, Npr1, Nr4a1, Nr4a2, Plcb1
Insulin secretion	Up	<0.01	6	2.018616571	Atp1b1, Atp1b3, Camk2d, Kcnmb3, Plcb1, Stx1a
Focal adhesion	Down	<0.01	31	4.770458001	Arhgap35, Capn2, Cav1, Col4a1, Col9a1, Dock1, Flnb, Flt1, Grb2, Igf1, Itga6, Itga7, Itga8, Itgb1, Lamc1, Mapk1, Mapk8, Pak4, Pdgfra, Pdgfrb, Pgf, Pik3cb, Rock2, Shc1, Shc2, Sos2, Thbs2, Tln1, Vav2, Vav3, Vcl
MAPK signaling pathway	Down	<0.01	36	4.569498466	Cacna1b, Chuk, Dusp3, Dusp7, Flnb, Grb2, Map3k2, Map3k3, Map3k4, Map3k6, Map3k7, Mapk1, Mapk14, Mapk8, Mapkapk2, Nfatc1, Nfatc3, Nr4a1, Ntrk2, Pdgfra, Pdgfrb, Rapgef2, Rela, Rps6ka2, Rps6ka4, Rras, Sos2, Srf, Stk3, Stk4, Stmn1, Tab le2, Tgfb2, Tgfbr1, Tgfbr2, Traf6
PI3K-Akt signaling pathway	Down	<0.01	41	3.691460714	Ccne2, Cdk6, Chuk, Col4a1, Col9a1, Efna1, Epha2, Flt1, Ghr, Gnb2, Gng11, Gng2, Grb2, Ifnar1, Igf1, Il2ra, Il7, Irs1, Itga6, Itga7, Itga8, Itgb1, Kitlg, Lamc1, Lpar3, Mapk1, Nr4a1, Pdgfra, Pdgfrb, Pgf, Pik3cb, Pkn2, Prlr, Rela, Rheb, Sgk1, Sos2, Tcl1a, Thbs2, Ywhab, Ywhag
Tight junction	Down	<0.01	25	3.689473532	Arhgap17, Arhgef18, Cldn10, Cttn, Hspa4, Itgb1, Jam2, Llgl2, Mapk8, Mpdz, Myh1, Myh10, Myh9, Myh9l1, Nedd4, Ocln, Pard3, Prkag2, Rapgef2, Rock2, Scrib, Tiam1, Tjp2, Tuba1b, Ybx3
Ras signaling pathway	Down	<0.01	31	3.654769244	Chuk, Efna1, Epha2, Exoc2, Flt1, Foxo4, Gnb2, Gng11, Gng2, Grb2, Igf1, Kitlg, Mapk1, Mapk8, Pak4, Pdgfra, Pdgfrb, Pgf, Pik3cb, Plcg1, Ralbp1, Ralgds, Rela, Rgl2, Rras, Shc1, Shc2, Sos2, Stk4, Tbk1, Tiam1

carbachol and adrenaline can promote the permeability of tight junctions and increase water transport through the paracellular pathway, and thus play a role in promoting secretion (Murakami et al., 2001). Inflammatory factors, such as TNF-α and IFN-γ, can destroy the integrity of the tight junctions between salivary gland epithelial cells, hinder the establishment of normal ion gradients and reduce salivary secretion (Baker et al., 2008). On the other hand, the MAPK pathway is a classic pathway that regulates the expression and function of tight junction proteins and is involved in a variety of tissues. Studies in the gastrointestinal tract have shown that somatostatin can protect the intestinal epithelium from the destruction of tight junctions induced by lipopolysaccharide by inhibiting the ERK1/2 pathway to downregulate the expression of somatostatin receptor 5 (Lei et al., 2014). Indomethacin can cause damage to the gastric epithelial barrier by activating the p38 pathway and reducing the expression of occludin (Thakre-Nighot and Blikslager, 2016). Moreover, the ERK1/2 pathway has also been reported in the reproductive system to regulate the formation of the blood epididymal barrier and to affect the expression and distribution of tight junction proteins (Kim and Breton, 2016). In general, the MAPK pathway and tight junction pathway are both closed to regulate salivary secretion. We found significant changes in the MAPK pathway and tight junction pathway in this study and suggested the following: on the one hand, BTXA might affect the MAPK pathway to regulate salivary secretion; on the other hand, BTXA probably inhibits salivary secretion by affecting the expression and distribution of tight junction proteins, and the MAPK pathway might also be involved. In addition, this KEGG analysis was performed based on the target genes of DE miRNAs, so miRNAs might play a role by affecting these two pathways in the process of BTXA inhibition of salivary secretion.

In addition, GO and KEGG analyses of DE mRNAs were performed to clarify the function of DE mRNAs. The cytokine-cytokine receptor interaction pathway was involved in the KEGG analysis of up- and downregulation of mRNAs, suggesting that this pathway may have an important role in inhibiting salivary secretion triggered by BTXA. Many past studies have shown that BTXA is closely related to the regulation of cytokine expression, especially in the process of regulating gland secretion. For example, BTXA injection into the submandibular gland after radiotherapy can alleviate the atrophy of the gland caused by radiotherapy and reduce the expression level of chemokine (C-X-C

motif) ligand 5 (Zeidan et al., 2016). After BTXA was injected into the lacrimal gland of rabbits, lacrimal secretion decreased and epidermal growth factor expression increased (Kim and Baek, 2013). After injecting 17.5 U BTXA into the lacrimal gland, the levels of IL-6 and IL-17 decreased significantly, and the patient's ocular surface condition was improved (Lu et al., 2014). Therefore, our study suggested that BTXA might change the expression level of cytokines and that these changes probably played a role in inhibiting the secretion of glands, but the specific effects need further study.

More importantly, we established a miRNA-mRNA network to clarify the specific relationship between them. We obtained seven mRNAs after the intersection of predicted miRNA target genes and DE mRNAs detected from the microarray, namely: Egr2, Paqr9, Zkscan1, Usp6nL, Cyb561a3, Zfhx4 and Clic5. The results were verified by qRT-PCR, demonstrating that these seven mRNAs changed authentically and reliably after BTXA injection into the submandibular gland, and these DE mRNAs were regulated by miRNAs. Clic5 is a member of the chloride intracellular channel family. The main function of Clic5 is to insert into the cell membrane, forming poorly selective ion channels that transport chloride ions (Bradford et al., 2010). In addition, this process is also necessary for the normal formation of stereocilia in the inner ear and development of the organ of Corti (Gagnon et al., 2006). In this study, we also queried the DAVID 6.8 database and performed GO analysis. The results demonstrated Clic5 was mainly involved in the molecular function domain, voltage-gated ion channel activity and chloride channel activity. In the biological process domain, the main GO terms included chloride transport, regulation of ion transmembrane transport, and chloride transmembrane transport. In the cell composition domain, the main GO terms included ion channels and chloride channels. Salivary secretion is the process of water and electrolyte molecule transport through the transcellular pathway and paracellular pathway. Therefore, when BTXA was injected into the rat submandibular gland, the decrease in Clic5 expression probably changed transepithelial ion absorption and secretion and finally affected the salivary secretion. According to our prediction results of target genes, Clic5 expression was regulated by rno-miR-122-5p. Therefore, we speculated that the expression of rno-miR-122-5p increased after BTXA injection into the submandibular gland, and then the expression of Clic5 was inhibited, thus affecting the transport of ions and finally inhibiting the secretion of submandibular
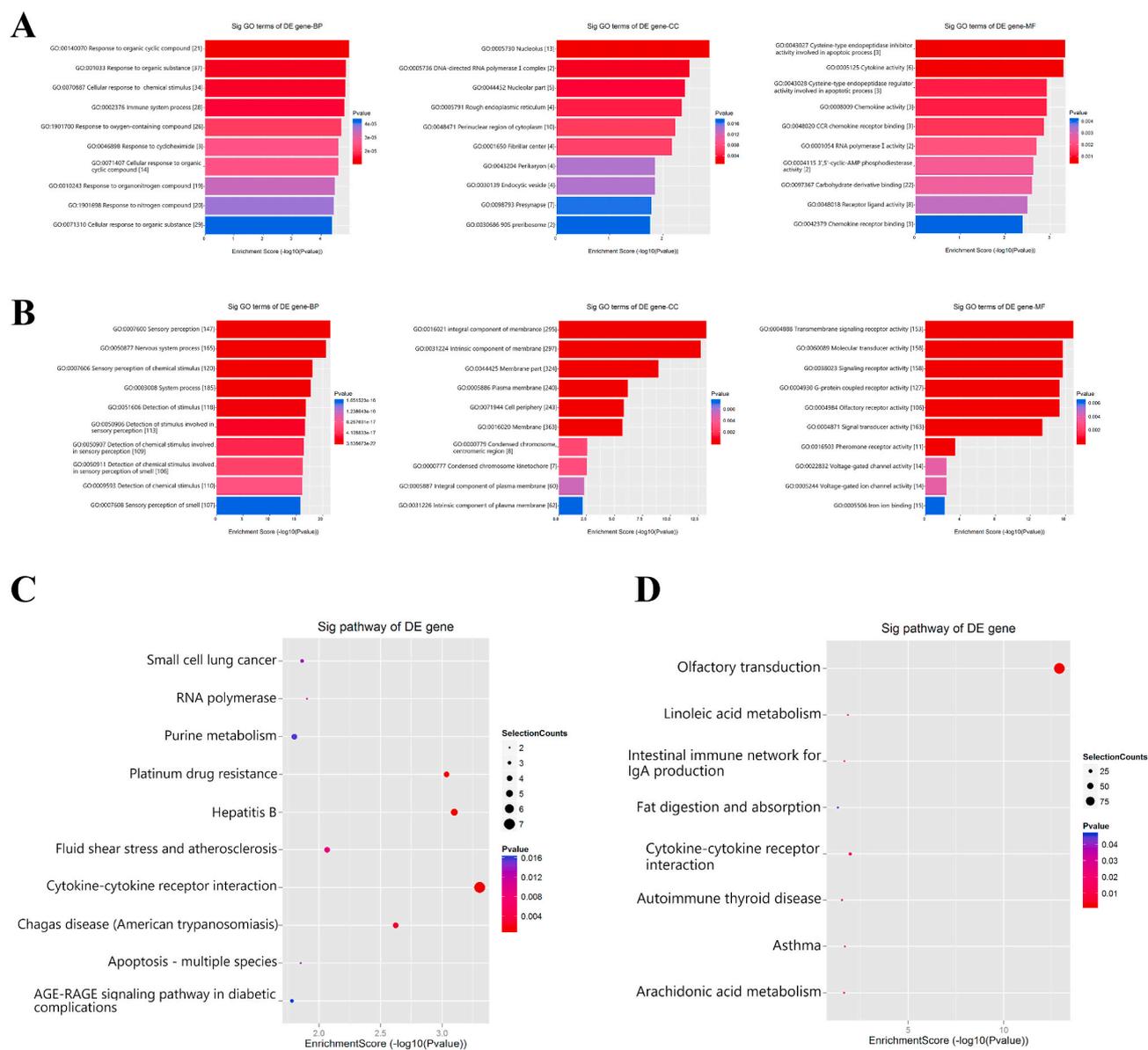
Fig. 4. GO and KEGG pathway analysis of DE mRNAs. A total of 743 DE mRNAs were chosen in the GO and KEGG analysis. (A) The top 10 GOs from upregulated mRNAs. (B) The top 10 GOs from downregulated mRNAs. Top 10 pathways from the KEGG pathway analysis of upregulated mRNAs (C) and downregulated mRNAs (D). DE, differentially expressed.

gland.

It is well known that BTXA inhibits the release of acetylcholine through cleavage of the synaptosome-associated protein 25. However, the previous studies identify that BTXA could affect the expression of miRNAs. BTXA directly inhibits the proliferation and migration of the keloid-derived fibroblast and promotes apoptosis and autophagy by regulating miR-1587/miR-2392 targeted ZEB2 (Hou et al., 2019). The expression of miR-133a/b, miR-1 and miR-206 alter in skeletal muscle following BTXA-induced muscle paralysis (Worton et al., 2018). Similarly, we found the aberrantly expressed miRNAs and mRNAs during BTXA inhibiting salivary secretion. MiRNAs are transcribed as pri-miRNAs and subsequently cleaved by the endoribonucleases Drosha and Dicer (Winter et al., 2009). Many factors could affect the miRNA biogenesis, among which the MAPK signalling pathway is one. DGCR8, a double-stranded RNA-binding protein, compose the microprocessor complex. It can be phosphorylated by ERK/MAPK, which leads to increased microprocessor complex activity and miRNA levels (Herbert et al., 2013). MiRNA-generating complex is comprised of Dicer and phospho-TRBP isoforms. TRBP is phosphorylated by the ERK/MAPK, which enhances miRNA production through the increasing stability of the Dicer–TRBP complex (Paroo et al., 2009). MAPK p38 and its downstream effector MAPK-activated protein kinase 2 are necessary for phosphorylates the auxiliary microprocessor component p68, which promotes the processes of pri-miRNAs (Hong et al., 2013). Meanwhile, it is reported that BTXA could activate the ERK/MAPK and p38 pathway (Kim et al., 2015; Miyashita et al., 2013). Therefore, we speculate that BTXA may affect miRNA biogenesis in the submandibular gland by affecting the MAPK pathway. However, we need more experiments to verify the specific mechanism.

Comprehensive analysis shows that miRNAs play an important role in the inhibitory effect of BTXA on submandibular gland secretion and our study provides a new idea for the mechanism of BTXA. However, the sample size of this study was relatively small, and the roles played by these genes in inhibitory effect of BTXA on salivary secretion remain to be further verified using the latest molecular biology techniques and systematic experiments in vivo and in vitro.
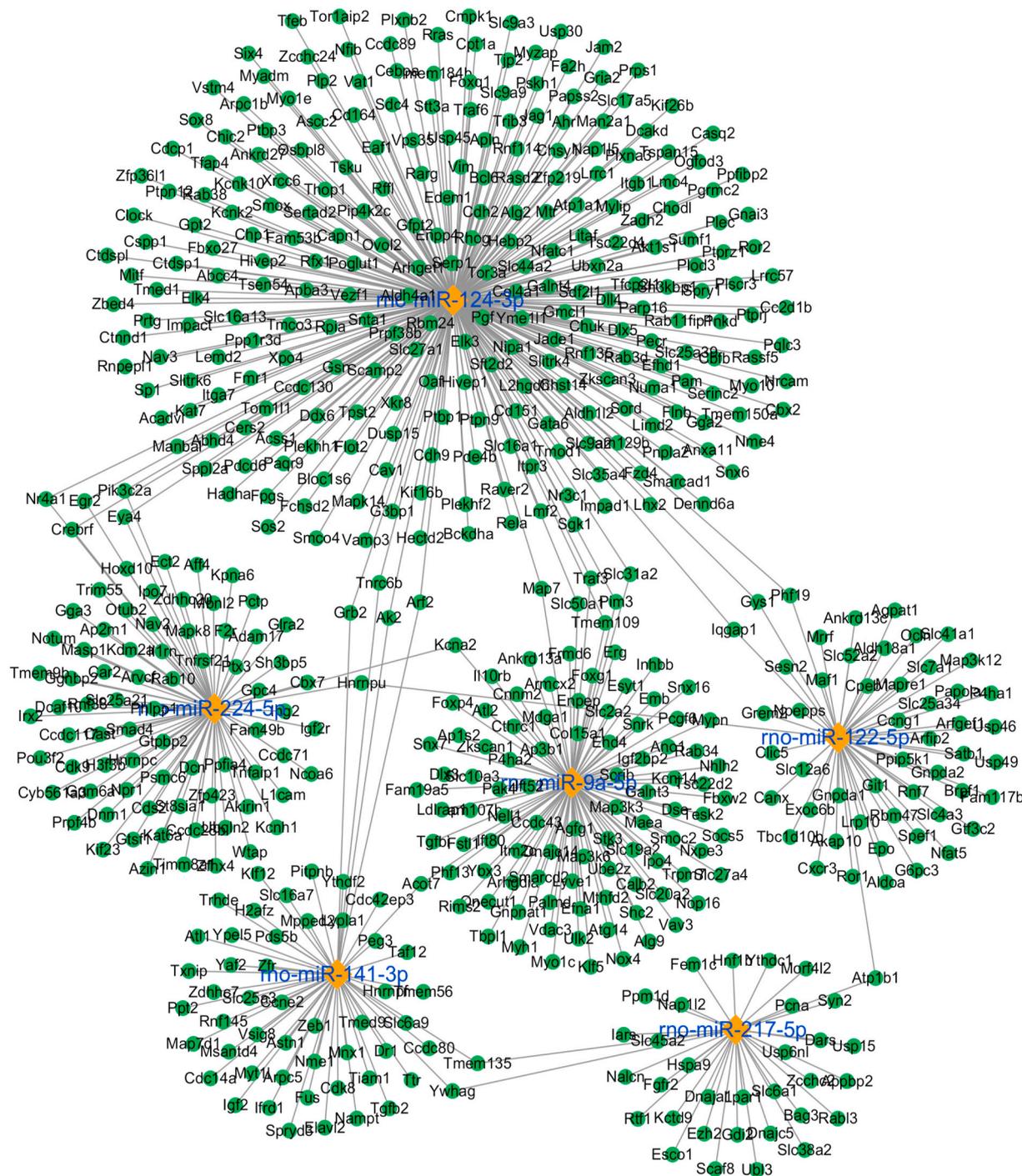
Fig. 5. miRNA-mRNA interaction network. Green circular nodes representing mRNAs, orange rectangular nodes representing miRNAs, and the association between them is plotted in solid lines. (For interpretation of the references to colour in this figure legend, the reader is referred to the Web version of this article.)

5. Conclusions

Our study describes the miRNA and mRNA expression profiles and functional network after injection of BTXA into the submandibular gland. We obtained several important miRNAs (miR-122-5p, rno-miR-217-5p, rno-miR-224-5p, rno-miR-124-3p, rno-miR-9a-5p and rno-miR-141-3p) after the injection of BTXA. Furthermore, the MAPK pathway and tight junctions which are most likely related to the inhibition of salivary secretion were more enriched. A miRNA-mRNA network was established to explore the relationship between them. These findings further explore the mechanism of BTXA in inhibiting salivary secretion and probably provide new ideas for clinical application.

Credit author statement

Qian-Ying Ma: Conceptualization, Data curation, Investigation, Methodology, Project administration, Writing – original draft, Shang Xie; Data curation, Investigation, Methodology, Validation, Writing – review & editing, Li-Ling Wu: Formal analysis, Resources, Validation, Visualization, Writing – review & editing, Ruo-Lan Xiang: Conceptualization, Funding acquisition, Resources, Supervision, Writing – review &

A

Venn diagram

566 7 1065

- Target genes of 7 miRNAs confirmed
- DE mRNAs

B
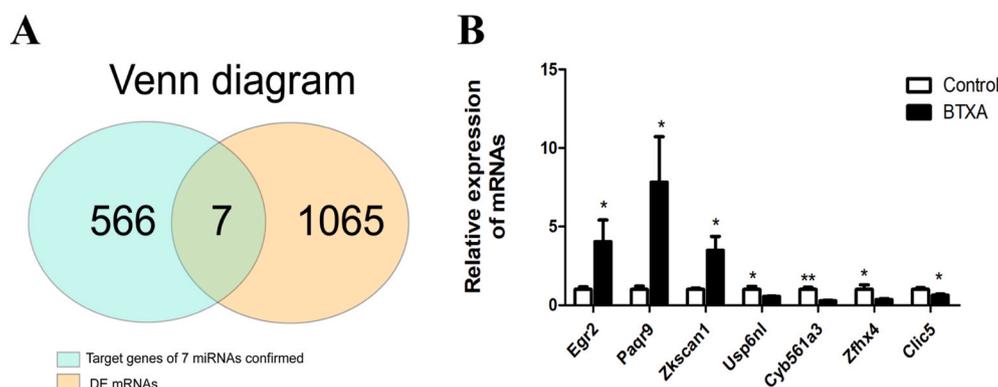
Fig. 6. Analysis of miRNA target mRNAs. (A) Venn diagram showing DE mRNAs and target genes of DE miRNAs (B) Validation of seven intersection mRNAs of target genes predicted by six DE miRNAs and DE mRNAs. N = 6–7/group, *P < 0.05 **P < 0.01. Egr2, early growth response 2; Paqr9, progestin and adipoQ receptor family member 9; Zkscan1, zinc finger with KRAB and SCAN domains 1; Usp6nl, USP6 N-terminal like; Cyb561a3, cytochrome *b*561 family member A3; Zfhx4, zinc finger homeobox 4; Clic5, chloride intracellular channel 5; DE, differentially expressed.

Table 2
The general information of seven mRNAs.

miRNA		Target genes				
Mature ID	Regulation	Gene symbol	Genbank accession	Regulation	Fold change	*P*-value
rno-miR-124-3p	Down	Egr2	NM 053633	Up	2.7981869	0.018
		Paqr9	NM 001271152	Up	2.7820273	0.013
rno-miR-9a-5p	Down	Zkscan1	NM 001025760	Up	2.2602869	<0.01
rno-miR-217-5p	Up	Usp6nl	NM 001106120	Down	3.2808614	<0.01
rno-miR-224-5p	Up	Cyb561a3	NM 001014164	Down	2.6880131	<0.01
		Zfhx4	NM 001191702	Down	2.3039056	<0.01
rno-miR-122-5p	Up	Clic5	NM 053603	Down	2.6565143	<0.01

Appendix A. Supplementary data

Supplementary data to this article can be found online at https://doi.org/10.1016/j.toxicon.2021.05.011.

Availability of data and material

The data that support the findings of this study are available at the National Center for Biotechnology Information Gene Expression Omnibus under accession number GSE141815 and GSE141819. Addresses are as follows:

https://www.ncbi.nlm.nih.gov/geo/query/acc.cgi?acc=GSE141815

https://www.ncbi.nlm.nih.gov/geo/query/acc.cgi?acc=GSE141819.

References

Baker, O.J., Camden, J.M., Redman, R.S., Jones, J.E., Seye, C.I., Erb, L., Weisman, G.A., 2008. Proinflammatory cytokines tumor necrosis factor-alpha and interferon-gamma alter tight junction structure and function in the rat parotid gland Par-C10 cell line. Am. J. Physiol. Cell Physiol. 295, C1191–C1201.

Banfi, P., Ticozzi, N., Lax, A., Guidugli, G.A., Nicolini, A., Silani, V., 2015. A review of options for treating sialorrhea in amyotrophic lateral sclerosis. Respir. Care 60, 446–454.

Barbero, P., Busso, M., Artusi, C.A., De Mercanti, S., Tinivella, M., Veltri, A., Durelli, L., Clerico, M., 2016. Ultrasound-guided botulinum toxin-A injections: a method of treating sialorrhea. JoVE (117), e54606.

Bradford, E.M., Miller, M.L., Prasad, V., Nieman, M.L., Gawenis, L.R., Berryman, M., Lorenz, J.N., Tso, P., Shull, G.E., 2010. CLIC5 mutant mice are resistant to diet-induced obesity and exhibit gastric hemorrhaging and increased susceptibility to torpor. Am. J. Physiol. Regul. Integr. Comp. Physiol. 298, R1531–R1542.

Chermansky, C.J., Kadow, B.T., Kashyap, M., Tyagi, P., 2018. MicroRNAs as potential biomarkers to predict the risk of urinary retention following intradetrusor onabotulinumtoxin-A injection. Neurourol. Urodyn. 37, 99–105.

Cong, X., Zhang, Y., Li, J., Mei, M., Ding, C., Xiang, R.L., Zhang, L.W., Wang, Y., Wu, L.L., Yu, G.Y., 2015. Claudin-4 is required for modulation of paracellular permeability by muscarinic acetylcholine receptor in epithelial cells. J. Cell Sci. 128, 2271–2286.

Gagnon, L.H., Longo-Guess, C.M., Berryman, M., Shin, J.B., Saylor, K.W., Yu, H., Gillespie, P.G., Johnson, K.R., 2006. The chloride intracellular channel protein CLIC5 is expressed at high levels in hair cell stereocilia and is essential for normal inner ear function. J. Neurosci. 26, 10188–10198.

He, Q., Zhou, X., Li, S., Jin, Y., Chen, Z., Chen, D., Cai, Y., Liu, Z., Zhao, T., Wang, A., 2013. MicroRNA-181a suppresses salivary adenoid cystic carcinoma metastasis by targeting MAPK-Snai2 pathway. Biochim. Biophys. Acta 1830, 5258–5266.

Herbert, K.M., Pimienta, G., DeGregorio, S.J., Alexandrov, A., Steitz, J.A., 2013. Phosphorylation of DGCR8 increases its intracellular stability and induces a progrowth miRNA profile. Cell Rep. 5, 1070–1081.

Hong, S., Noh, H., Chen, H., Padia, R., Pan, Z.K., Su, S.B., Jing, Q., Ding, H.F., Huang, S., 2013. Signaling by p38 MAPK stimulates nuclear localization of the microprocessor component p68 for processing of selected primary microRNAs. Sci. Signal. 6, ra16.

Hou, Z., Fan, F., Liu, P., 2019. BTXA regulates the epithelial-mesenchymal transition and autophagy of keloid fibroblasts via modulating miR-1587/miR-2392 targeted ZEB2. Biosci. Rep. 39.

Kapsogeorgou, E.K., Papageorgiou, A., Protogerou, A.D., Voulgarelis, M., Tzioufas, A.G., 2018. Low miR200b-5p levels in minor salivary glands: a novel molecular marker predicting lymphoma development in patients with Sjogren's syndrome. Ann. Rheum. Dis. 77, 1200–1207.

Kim, B., Breton, S., 2016. The MAPK/ERK-Signaling pathway regulates the expression and distribution of tight junction proteins in the mouse proximal epididymis. Biol. Reprod. 94, 22.

Kim, J.W., Baek, S., 2013. Functional and histologic changes in the lacrimal gland after botulinum toxin injection. J. Craniofac. Surg. 24, 1960–1969.

Kim, Y.J., Kim, J.H., Lee, K.J., Choi, M.M., Kim, Y.H., Rhie, G.E., Yoo, C.K., Cha, K., Shin, N.R., 2015. Botulinum neurotoxin type A induces TLR2-mediated inflammatory responses in macrophages. PloS One 10, e0120840.

Lei, S., Cheng, T., Guo, Y., Li, C., Zhang, W., Zhi, F., 2014. Somatostatin ameliorates lipopolysaccharide-induced tight junction damage via the ERK-MAPK pathway in Caco2 cells. Eur. J. Cell Biol. 93, 299–307.

Lu, R., Huang, R., Li, K., Zhang, X., Yang, H., Quan, Y., Li, Q., 2014. The influence of benign essential blepharospasm on dry eye disease and ocular inflammation. Am. J. Ophthalmol. 157, 591–597.

Martini, D., Gallo, A., Vella, S., Sernissi, F., Cecchettini, A., Luciano, N., Polizzi, E., Conaldi, P.G., Mosca, M., Baldini, C., 2017. Cystatin S-a candidate biomarker for severity of submandibular gland involvement in Sjogren's syndrome. Rheumatology 56, 1031–1038.

Mei, M., Xiang, R.L., Cong, X., Zhang, Y., Li, J., Yi, X., Park, K., Han, J.Y., Wu, L.L., Yu, G. Y., 2015. Claudin-3 is required for modulation of paracellular permeability by TNF-alpha through ERK1/2/slug signaling axis in submandibular gland. Cell. Signal. 27, 1915–1927.

Miyashita, S., Sagane, Y., Inui, K., Hayashi, S., Miyata, K., Suzuki, T., Ohyama, T., Watanabe, T., Niwa, K., 2013. Botulinum toxin complex increases paracellular permeability in intestinal epithelial cells via activation of p38 mitogen-activated protein kinase. J. Vet. Med. Sci. 75, 1637–1642.

Mohr, A.M., Mott, J.L., 2015. Overview of microRNA biology. Semin. Liver Dis. 35, 3–11.

Murakami, M., Shachar-Hill, B., Steward, M.C., Hill, A.E., 2001. The paracellular component of water flow in the rat submandibular salivary gland. J. Physiol. 537, 899–906.

Paroo, Z., Ye, X., Chen, S., Liu, Q., 2009. Phosphorylation of the human microRNA-generating complex mediates MAPK/Erk signaling. Cell 139, 112–122.

Restivo, D.A., Panebianco, M., Casabona, A., Lanza, S., Marchese-Ragona, R., Patti, F., Masiero, S., Biondi, A., Quartarone, A., 2018. Botulinum toxin A for sialorrhoea associated with neurological disorders: evaluation of the relationship between effect of treatment and the number of glands treated. Toxins 10.

Slawek, J., Madalinski, M., 2017. Botulinum toxin therapy for nonmotor aspects of Parkinson's disease. Int. Rev. Neurobiol. 134, 1111–1142.

Srivanitchapoom, P., Pandey, S., Hallett, M., 2014. Drooling in Parkinson's disease: a review. Park. Relat. Disord. 20, 1109–1118.

Thakre-Nighot, M., Blikslager, A.T., 2016. Indomethacin induces increase in gastric epithelial tight junction permeability via redistribution of occludin and activation of p38 MAPK in MKN-28 Cells. Tissue Barriers 4, e1187325.

Walshe, M., Smith, M., Pennington, L., 2012. Interventions for drooling in children with cerebral palsy. Cochrane Database Syst Rev, p. CD008624.

Winter, J., Jung, S., Keller, S., Gregory, R.I., Diederichs, S., 2009. Many roads to maturity: microRNA biogenesis pathways and their regulation. Nat. Cell Biol. 11, 228–234.

Worton, L.E., Gardiner, E.M., Kwon, R.Y., Downey, L.M., Ausk, B.J., Bain, S.D., Gross, T. S., 2018. Botulinum toxin A-induced muscle paralysis stimulates Hdac4 and differential miRNA expression. PloS One 13, e0207354.

Xie, S., Xu, H., Shan, X.F., Cai, Z.G., 2019. Botulinum toxin type A interrupts autophagic flux of submandibular gland. Biosci. Rep. 39.

Xu, H., Shan, X.F., Cong, X., Yang, N.Y., Wu, L.L., Yu, G.Y., Zhang, Y., Cai, Z.G., 2015. Pre- and post-synaptic effects of botulinum toxin A on submandibular glands. J. Dent. Res. 94, 1454–1462.

Yang, Y., Peng, L., Ma, W., Yi, F., Zhang, Z., Chen, H., Guo, Y., Wang, L., Zhao, L.D., Zheng, W., Li, J., Zhang, F., Du, Q., 2016. Autoantigen-targeting microRNAs in Sjogren's syndrome. Clin. Rheumatol. 35, 911–917.

Zeidan, Y.H., Xiao, N., Cao, H., Kong, C., Le, Q.T., Sirjani, D., 2016. Botulinum toxin confers radioprotection in murine salivary glands. Int. J. Radiat. Oncol. Biol. Phys. 94, 1190–1197.